\$ SUPER

Contents lists available at ScienceDirect

Results in Chemistry

journal homepage: www.sciencedirect.com/journal/results-in-chemistry





Chloramphenicol-infused N-vinyl-based soft contact lenses for therapeutic and optical applications

Lina M. Shaker ^{a,*}, Ahmed Alamiery ^{a,b}, Abdulamier Ahmed Abdulamier ^c, Wan Nor Roslam Wan Isahak ^b

- ^a Al-Ayen Iraqi University Nasiriyah Iraq
- b Department of Chemical and Process Engineering Faculty of Engineering and Built Environment University Kebangsaan MalaysiaMalaysia (UKM) Bangi P.O. Box 43000 Selansor Malaysia
- ^c College of Pharmacy, Al-Farahidi University, Baghdad 10001 Iraq

ARTICLE INFO

Keywords: Soft contact lenses Drug delivery Biocompatibility Chloramphenicol Nanomaterials

ABSTRACT

This work is exploring the development of antibacterial contact lenses (CLs) by implementing the silicon-N-vinyl pyrrolidone-2-hydroxyethyl methacrylate (Si-NVP-HEMA) base to combat the corneal bacterial infections. Due to its hydrophilic and flexible properties, Si-NVP-HEMA enhances oxygen permeability and allows for more effective pairing with antibacterial agents. The lenses were infused with chloramphenicol (CAM) and in some cases, additives like silver and titanium dioxide nanoparticles (Ag and TiO2 NPs) were added to boost their antibacterial capabilities. Key analysis including UV-Vis spectra, refractive index (RI) measurement, scanning electron microscopy (SEM) images, and Fourier-transform infrared (FTIR) charts confirmed the lenses' physical, chemical, and therapeutic performance. The fabricated lenses demonstrated an impressive RI range of 1.49 to 1.53 preserving visual clarity and achieving over 95% visible light transmittance while effectively blocking UV radiation. Antibacterial testing revealed significant enhancements in effectiveness against certain bacteria, including Staphylococcus aureus and Escherichia coli (S. aureus and E. coli). This promising formulation shows merit as a safe, comfortable, and extended use CL option by providing comprehensive protection, excellent optical performance, and essential properties like water content and oxygen permeability. This Si-NVP-HEMA based formulation provides a multifunctional solution integrating antimicrobial protection UV blocking capabilities and excellent optical performance with essential water content and oxygen permeability positioning it as a promising option for safe comfortable extended wear CLs.

Introduction

With the number of contact lens (CL) wearers projected to grow to over 150 million worldwide, the therapeutic role of these lenses represents a significant opportunity in ophthalmology [1]. The increasing prevalence of myopia globally, affecting approximately 1.45 billion people, has underscored the need for therapeutic interventions. CLs serve as controlled drug delivery platforms [2]. As highlighted by Chandel A and Kandav G (2024), CLs address the limitations of common treatments like eye drops, ointment, which suffer from low bioavailability, short retention times, and related side effects [3]. The integration of nanomaterials and innovative polymer systems offers improved patient compliance by enhancing drug permeability extend release

durations, improve therapeutic efficacy, and reducing dosage frequency [4]. For CLs to fulfill their therapeutic function, they must allow the passage of water, oxygen, and drugs, maintaining a favorable environment for corneal health and aerobic metabolism. Manufacturers have incorporated siloxane groups (Si-O-Si) into hydrogels to optimize these properties, especially in silicone lenses [5]. In addition, methods such as salt-induced modulation have been shown to increase drug loading efficiency in CLs without affecting optical transparency, a key factor in maintaining visual quality during therapy. According to Zhu and Mao (2019), drug loading efficiency in CLs can be significantly improved by salt-induced modulation [6]. Zhao et al. (2023) explore various drug delivery techniques through CLs, including chemical cross-linking and the use of nanoparticles (NPs) to prolong drug release and improve

E-mail addresses: linamohmmed91@gmail.com (L.M. Shaker), dr.ahmed1975@ukm.edu.my (A. Alamiery), wannorroslam@ukm.edu.my (W.N. Roslam Wan sahak).

^{*} Corresponding author.

retention [7]. CL discomfort remains a primary reason for discontinuation among wearers, as highlighted by Rueff (2023) [8], and Costa et al. (2024) [9]. Rueff (2023) suggests that visual factors, including vision-related disorders, may play a significant role in discomfort, as these disorders share symptoms with those experienced by CL wearers. Meanwhile, Costa et al. (2024) focus on the physical properties of lens materials, noting that the coefficient of friction on CL surfaces impacts tear film stability and lubrication. According to Tam, Alexander, Sanderson, and Qi (2024), the selective coating technique using nanoelectrospray on CLs has been used to create drug-eluting CLs (DECLs) for the treatment of ocular diseases [10].

The use of advanced materials and techniques to develop innovative CLs with therapeutic properties. Specifically biocompatible polymers like poly(vinyl alcohol) (PVA) are a solution, and poly(vinyl pyrrolidone) (PVP) are used to prepare hydrogels widely for wearable medical applications [11]. Additionally, PVA is water soluble where the hydroxyl [-OH] group bonding with alternating carbon atom, and as such, it is categorized as hydrophilic material [12]. The PVP-PVA blends have emerged as a new tool for biomaterial devices preparations [13]. There is previous evidence that the PVA polymer can be filled with the required drugs when it is manufactured [14]. In addition, PVA hydrogels demonstrates significant potential for integration with nanomaterials such as silver NPs [15], or drug loaded chitosan NPs [16], as seen in their application for antibacterial purposes and drug delivery systems. Despite advances in therapeutic CLs, some challenges remain. One of them is the development of effective methods to control drug release, as many conventional CL materials do not allow for prolonged release without affecting comfort and transparency. Designing therapeutic CLs with high refractive index (RI; that mathematically symbolled by n) and high oxygen permeability is essential to ensure that visual clarity is maintained without compromising corneal health. Recent trials have proposed the use of hybrid CLs and composite materials combining PVA and PVP, which not only allow drug loading but also enhance the mechanical properties [17]. Peili Zhao (2018) proposed ZnS-inorganic hydrogel CLs by copolymerizing ZnS with 2-hydroxyethyl methacrylate (HEMA), achieving n values from 1.38 to 1.45 as ZnS content ranged from 30 % to 60 % [18]. Scott et al. (2018) developed Si-based rigid gas permeable CLs with a liquid crystal layer between two rigid polymer layers (n \approx 1.43) [19]. That year, J. Schafer and colleagues integrated SiHy CLs with PVP, creating smooth, water-preserved lenses for long computer use [20].

Despite advancements in sustainable drug-infused CLs, achieving consistent antibacterial efficacy, high transparency, and UV blocking within a single CL remains challenging [21]. Current studies on N-vinyl-based materials focus on enhancing drug release and transparency [22], limited research addresses integrating chloramphenicol (CAM) with Ag and TiO₂ NPs to maximize antibacterial properties while maintaining corneal compatibility and high visible light transmission. Innovative approaches such as 3D electrohydrodynamic printing of CAM-loaded cellulose acetate patches offer promising solutions with sustained drug release highlight transmittance and biocompatibility demonstrating potential for corneal abrasion treatment. However, challenges like oxygen permeability's comfort and optical performance limit their broader application to conventional lenses highlighting the need for improved solutions to reduce ocular infection risks without compromising user experience.

This research aims to bridge this gap by developing CAM-infused N-vinyl-based soft CLs, designed to provide both therapeutic efficacy and optimal optical properties. By integrating antimicrobial agents such as CAM, the study seeks to reduce infection risks without compromising the essential performance attributes of CLs, such as oxygen permeability, hydration, and visual clarity. In doing so, it addresses the growing need for safe, effective, and comfortable CL options, especially for extended-wear users. Moreover, this research aligns with key Sustainable Development Goals (SDGs), particularly SDG 3: Good Health and Well-being, by improving ocular health and reducing the risk of eye infections. It

also contributes to SDG 9: Industry, Innovation, and Infrastructure, advancing the development of multifunctional medical devices, and has the potential to promote sustainable production practices within the medical device industry, in line with SDG 12: Responsible Consumption and Production.

Materials and method

Preparation of Si-NVP-HEMA base material

According to our previous review research entitled "Advancements in the chemistry of contact Lenses: Innovations and applications", the material composite was used in this work [23]. The experimental work was conducted to prepare polymerizable lens compositions and fabricate CLs using injection molding techniques.

The CLs compositions were formulated by mixing the ingredients listed in Fig. 1, each contributing specific functional roles. The formulation included 40 wt% Tetraethyl orthosilicate (TEOS) (1.20 g ≈ 1.28 mL), a Si-containing compound that provides the structural framework for mechanical stability and enhances oxygen permeability. Methacryloxypropyltris(trimethylsiloxy)silane (MOPTS), a Si-containing macromer comprising 11 wt% (0.33 g \approx 0.32 mL), further improves oxygen permeability and lens flexibility. The hydrophilic monomers, Nvinylpyrrolidone (NVP) and 2-hydroxyethyl methacrylate (HEMA), were incorporated at 30 wt% (0.90 g) and 15 wt% (0.45 g), respectively, to increase water retention and wettability, which are essential for wearer comfort. Ethyleneglycol dimethacrylate (EGDMA), at 2 wt% $(0.06 \text{ g} \approx 0.06 \text{ mL})$, acts as a crosslinking agent, ensuring the mechanical strength and durability of the polymer matrix. Lastly, the initiator 2,2'azobis(2-methylpropanenitrile) (VAZO®-64) was added at 2 wt% (0.06 g) to facilitate the polymerization process by initiating free radical reactions, leading to the formation of a stable polymer network.

The mixing process was carried out at room temperature for a duration of 5 h. The amide (N-C=O) group present in molecules exhibits significant polarity, facilitating the formation of hydrogen bonds with two water molecules. Because of this polarity, copolymers based on NVP deviate from the smooth and slippery sensation commonly associated with PHEMA and instead display a rubberier texture. Moreover, with a progressive rise in the concentration of NVP, the RI of the CL increases owing to the high molar refraction of the pyrrolidone ring within NVP [24]. Increasing NVP concentration in CLs raises RI, which, combined with reduced contrast sensitivity under low-light or glare conditions, may further impact visual clarity and performance for lens wearers [25]. CL molds were created via injection molding using non-polar polypropylene resin and standard equipment. The molds comprised a female member with a concave optical surface for the front lens shape and a male member with a convex optical surface for the back. Around $60\,\mu l$ of the polymerizable lens composition was deposited onto the female-mold concave surface, and then the male-mold was pressed onto it, filling the lens-shaped cavity, and left to dry. Mechanical demolding separated the molds, leaving the lens attached to the male-mold. Delensing carefully removed the lens from the male-mold. These steps included washing the lens product in ethanol, hydrating it in a sodium hyaluronate solution, and conducting different tests to characterize the hydrated CL product. This experimental approach allowed for the successful [1]. In fact, the most increased global prevalence eye disorder called myopia, affecting CLs wearers worldwide, where the associated risks to myopia have become a major public health concern [26].

Si-NVP-HEMA CLs loaded with TiO2 and Ag NPs

The preparation of NP-loaded CLs involved dissolving TiO_2 NPs (0.10 g) and Ag NPs (0.05 g) separately in 40 ml of ethanol at 70 °C under controlled stirring conditions for 60 min to ensure a uniform suspension. Prior to NP loading, all Si-NVP-HEMA CLs were treated with acetone solvent for 5 min to de-swell the polymer and prepare the

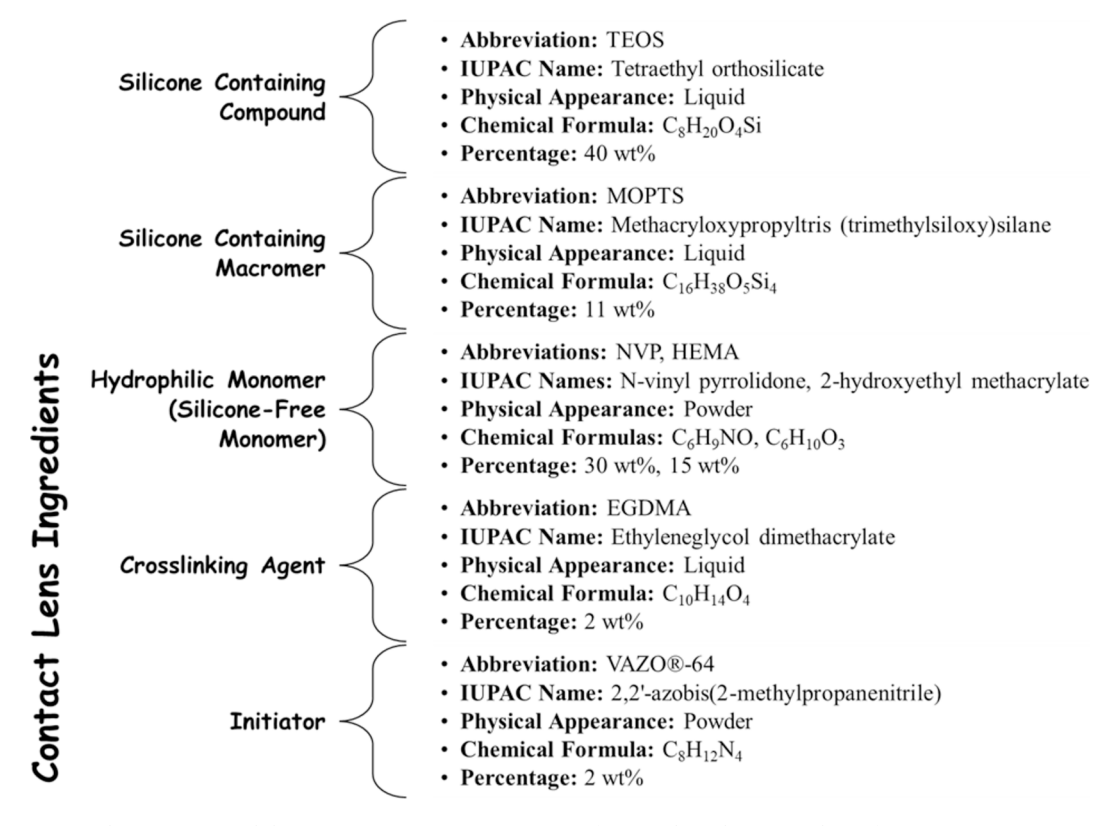


Fig. 1. Essential components and their precise compositions in creating functional Synthesis Ingredients for Si-NVP-HEMA CLs materials.

surface for efficient NP adhesion, as shown in Fig. 2a. These lenses were then distributed into divided petri dishes.

As shown in Fig. 2b and listed in Table 1, five Si-NVP-HEMA-based CLs were prepared as the T-group, organized by concentration from T1 to T5, by loading the front (outer) surface with TiO_2 NPs in varying

concentrations. After loading, the samples were left to dry for 24 h. Another set of five lenses was prepared as the A-group, organized by concentration from A1 to A5, as shown in the same image, by loading the inner surface with Ag NPs in concentrations specified in Table 2. These samples were also left to dry for 24 h. After drying, the T-group CLs were

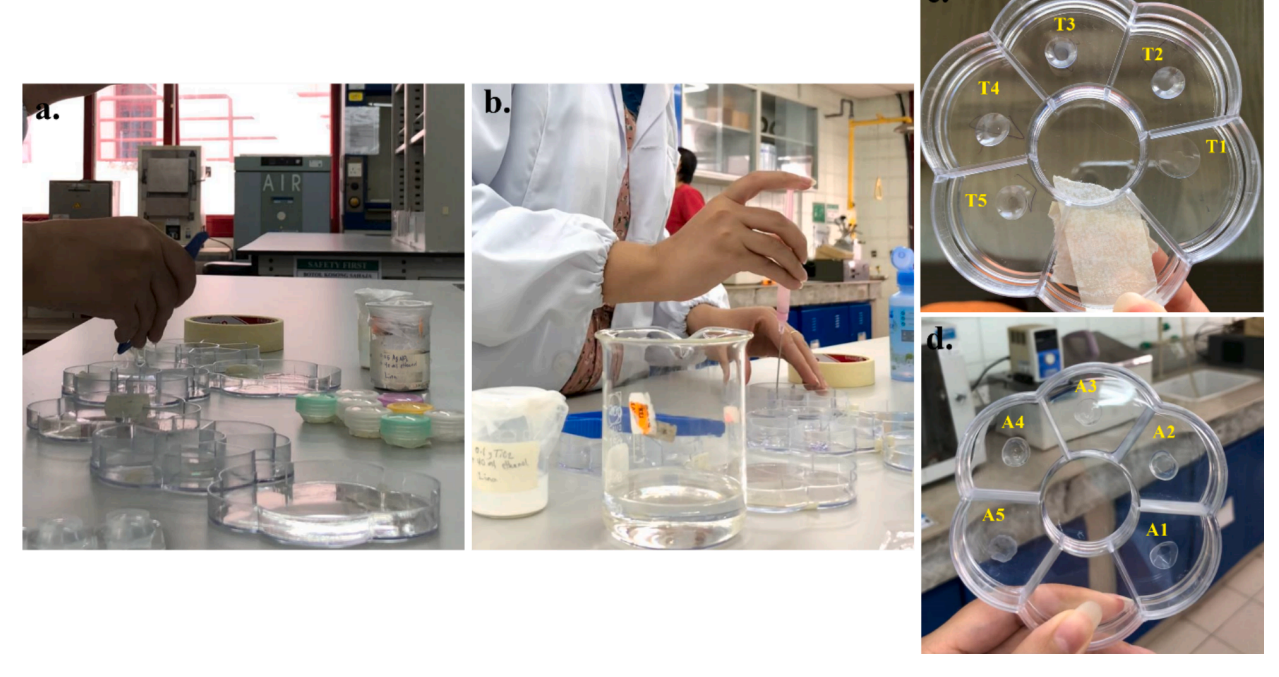


Fig. 2. A. preparing the synthesis dried si-nvp-hema cls by washing them with acetone to remove impurities, followed by distributing them into divided petri dishes. b. loading of tio₂ NPs (T-group) and Ag NPs (A-group) onto the lenses. c. CLs loaded with TiO₂ NPs, organized by concentration (T1–T5). d. CL loaded with Ag NPs, organized by concentration (A1–A5).

Table 1TiO₂ NPs concentrations loaded onto Si-NVP-HEMA CLs surfaces.

Preparation steps	Sample	Concentration (×10 ⁻³ wt/L)
0.10 g of TiO ₂ in 40 ml ethanol	Stock Solution	2.50×10^{-3}
0.50 ml of stock is diluted in 2.50 ml of ethanol	T1	0.50×10^{-3}
1 T1 concentration diluted in 2 ml of ethanol	T2	0.28×10^{-3}
1 T2 concentration diluted in 2 ml of ethanol	Т3	0.25×10^{-3}
1.50 T3 concentration diluted in 1 ml of ethanol	T4	0.19×10^{-3}
$1.50\mathrm{T4}$ concentration diluted in $1\mathrm{ml}$ of ethanol	T5	0.13×10^{-3}

Table 2Ag NPs concentrations loaded onto Si-NVP-HEMA CLs surfaces.

Preparation steps	Sample	Concentration (×10 ⁻³ wt/L)
0.05 g of Ag in 40 ml ethanol	Stock Solution	1.25×10^{-3}
0.50 ml of stock is diluted in 2 ml of ethanol	A1	0.31×10^{-3}
0.50 A1 concentration diluted in 2 ml of ethanol	A2	7.81×10^{-5}
0.50 A2 concentration diluted in 2 ml of ethanol	A3	1.95×10^{-5}
0.50 A3 concentration diluted in 2 ml of ethanol	A4	4.88×10^{-6}
0.50 A4 concentration diluted in 2 ml of ethanol	A5	1.22×10^{-6}

washed twice with ethanol to remove excess particles, as shown in Fig. 2c. The same procedure was followed for the A-group CLs, with the final products shown in Fig. 2d.

Loading CAM to CLs

CAM powder was purchased from Samarra Pharmaceutical Factory, Ibn Hayyan Factory Branch, Samarra, Iraq. 20 mg of CAM powder was accurately weighed and dissolved in 200 ml of ethanol, resulting in the preparation of a stock solution, where each milliliter (1 mL) contains an amount equivalent to 0.10 mg of CAM. Thus, the CAM stock solution concentration is 0.10 mg/mL. The potential benefits of CAM were then assessed on three pure and loaded Si-NVP-HEMA lenses incorporating Ag and TiO $_2$ NPs.

To assess antibacterial activity, three 3.20 mm diameter discs were punched from each lens using hole punch plier. The discs were immersed separately, in CAM solution for 3 h to ensure that the specimens inhaled the solution. These discs were then placed on nutrient agar plates inoculated with *Staphylococcus aureus* and *Escherichia coli* (*S. aureus (ATCC 25923)) and E. coli (ATCC 25922)*), respectively. After a 24 h incubation at 37 °C, the zones of inhibition were measured to determine the antimicrobial efficacy of the lens materials. Each test was conducted three times, and only the average was recorded to ensure accuracy and consistency. A statistical comparison was performed using one-way ANOVA (analysis of variance) to evaluate whether the mean inhibition zones across the test groups (Control, Pure, T4, A4) were significantly different.

Through a rigorous examination of these factors, valuable insights will be gained, shedding light on the potential applications and advantages of incorporating CAM in the loaded Si-NVP-HEMA lenses. These insights are poised to significantly contribute to the advancement of functional CL technology, offering wearers enhanced performance and improved eye health benefits.

Characterization of CLs groups

Scanning Electron Microscope Analysis

Scanning electron microscope is one of the most widely used instrumental methods for the examination and analysis of micro- and NP imaging characterization of solid objects. SEM topographical images were obtained with a ZEISS MERLIN microscope (i-CRIM, UKM, Selangor, Malaysia). The SEM images were conducted for the dried pure and NPs-loaded CLs groups.

Water content analysis and oxygen permeability measurement

The EWC of a hydrogel may vary depending on the environmental conditions. Most CL hydrogels will undergo a small change in EWC when placed in solutions of different pH and osmolality, but these changes will be most pronounced in ionic lens materials. The oxygen and ion permeability of a CL material are intimately associated with its EWC. Since the cornea receives most of its oxygen from the atmosphere, the oxygen transmissibility profile of a CL is one of its most important properties. Oxygen permeability is a property of the material itself and is described as the Dk, where D is the diffusivity of the material and k is the solubility of the material. Oxygen permeability is essentially governed by EWC in conventional hydrogels. This relationship is based on the ability of oxygen to pass through the water rather than through the material itself. To calculate the amount of oxygen which will move from the anterior to the posterior surface of a lens, the oxygen permeability in Dk is divided by the thickness (t) of the lens. The hydrated CLs were removed from the aqueous lens solution, wiped to remove excess surface water, and weighed. The lenses were then dried at room temperature for a couple of days and reweighed. The weight difference was calculated by subtracting the weight of the dry lens from the weight of the hydrated lens. The EWC (%) of the lenses was measured based on their weight before and after hydration, according to Equation (1), where gas permeability exponentially changes with water content as shown in Equations (2) and (3).

$$EWC = \frac{weight\ of\ hydrated\ lens-weight\ of\ dried\ lens}{weight\ of\ hydrated\ lens}\times\ 100 \eqno(1)$$

The EWC of a hydrogel is influenced by environmental conditions, pH, tonicity, and temperature. The International Organization for Standardization defines the regulatory standards for EWC measurements in CL hydrogels. Both thermogravimetry and back-calculation by RI measurements are considered valid techniques for EWC assessment.

The oxygen permeability is indicated as Dk, where D is the diffusivity and k is the solubility of the material [27]. Hydrogels transport oxygen via the water channels and their oxygen permeability is closely related to temperature and EWC, according to the following Equation:

$$DK = 1.67e^{0.0397 \times EWC} \tag{2}$$

The amount of oxygen transported from the anterior to the posterior surface O_2 , $A \rightarrow P$ of a lens can be calculated according to Equation 2.9 by dividing the oxygen permeability Dk by the lens thickness t:

$$O_2 = DK/t \tag{3}$$

Fourier transform infrared analysis

FT-IR Spectrometer is a versatile and invaluable tool in the analysis of organic compounds. Its ability to identify functional groups, determine molecular structures, and offer insights into chemical bonds makes it an essential instrument in various scientific fields and industries. The experimental work utilized the FT-IR with the model Spectrum 400 FT-IR/NIR and Imaging System (i-CRIM, UKM, Selangor, Malaysia). This equipment was employed to analyze the functional groups and chemical bonds present in molecules. The analysis was conducted using standard transmission mode on four samples of pure and NPs-loaded CLs after loading them with CAM.

Results and Discussions

Optical transparency and index of refraction

The absorption peaks, transmission percentage, RI and Abbe number trends observed in the CLs loaded with ${\rm TiO_2}$ and Ag NPs reflect the intricate interplay of NP type, concentration, and their unique optical characteristics. The presence of a silicon monomer absorption peak at 297 nm plays a crucial role in understanding the shifting of absorption peaks in the context of these CLs. The base polymer composite, which includes materials like TEOS and Methacryloxypropyltris (trimethylsiloxy)silane, contains Si-related compounds. These Si- compounds can contribute to the absorption behavior in the UV–visible spectrum.

T-group CLs

As shown in Fig. 3a, the absorption spectra of TiO_2 NP-loaded T-group samples demonstrate distinct characteristics that correlate strongly with NPs concentration within the lens material. As the concentration of TiO_2 NPs varies from T5 to T1, a corresponding shift in absorbance intensity is observed. T1 and T5 exhibit the highest absorbance values at 1.09 and 0.82, respectively. This intensity decreases for T3 (0.55) and T4 (0.59), though T2 (0.82) shows a higher absorbance than T4 despite a slightly lower concentration. The absorbance levels

may correlate with the size and distribution of the $\rm TiO_2$ NPs, where smaller NPs (approximately 21 nm) provide a larger surface area, potentially increasing absorbance [28]. The absorption peaks for CLs loaded with T1-T5 samples are consistently centered around 296–298 nm. Additionally, as $\rm TiO_2$ NP concentration decreases, the absorption peaks display a subtle blue shift, possibly due to the influence of Sicompounds in the base polymer composite. Si-based groups may affect the electron transition of $\rm TiO_2$ NPs or alter the electronic properties of the polymer matrix, leading to these peak shifts [29]. Consequently, reduced $\rm TiO_2$ concentrations may modify these interactions, contributing to the observed blue shift in absorption peaks.

Across T-group, transmittance generally decreases with increasing wavelength, a common phenomenon in the visible spectrum due to light absorption by the lens materials. Fig. 3.b illustrates the transmission spectra of T-group. Interestingly, despite having the highest TiO_2 NP concentration, CL T1 exhibits the highest transmission across the visible wavelength range. This counterintuitive observation can be explained by the concept of percolation. At higher NP concentrations, a network-like structure forms, facilitating light passage with less obstruction. In contrast, T2, with a lower TiO_2 NP concentration than T1, displays reduced transmission throughout the spectrum, aligning with the general trend of TiO_2 NPs decreasing light transmission. CLs T3 to T5 show a slight increase in transmission as TiO_2 NP concentration decreases. Additionally, factors like NP agglomeration or clustering in T2 and other

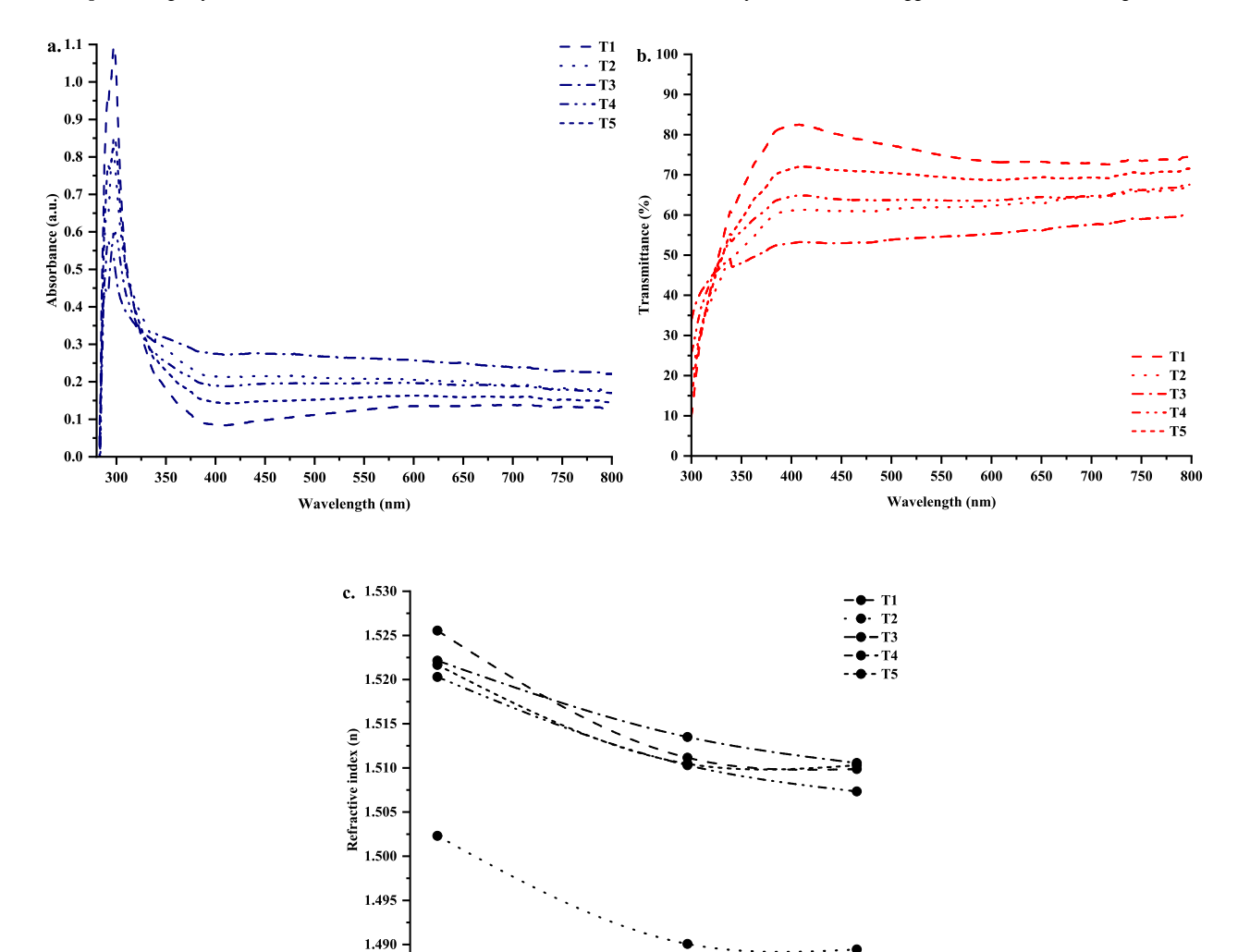


Fig. 3. A. uv-Vis absorption spectra, b. transmission rate spectra, and c. RI of T1-T5 CLs.

575

Wavelength (nm)

625

525

L.M. Shaker et al. Results in Chemistry 13 (2025) 102034

lenses may contribute to increased light scattering and reduced transmission.

T-group CLs exhibit a wavelength-dependent RI, as depicted in Fig. 3.c. This property is notably influenced by their dispersion coefficient, the Abbe number. Across T-group, RI values typically range between 1.50 and 1.53, with a subtle RI increase observed as TiO2 NP concentration decreases. This trend may result from the influence of NPs on optical properties of the materials, where higher TiO₂ concentrations create more pronounced effects. Beyond concentration, variables such as NP size, distribution, optical properties, agglomeration, and interactions within the polymer matrix play significant roles in the transmission spectra. Interestingly, T1 lenses achieve superior transmission despite higher TiO2 levels, likely due to a combination of these factors reducing light scattering effects. The RI behavior of T-group CLs, as a function of wavelength, exhibits a dispersion profile indicative of wavelength-dependent RI variations. This property has the potential to enhance visual performance. These findings corroborate our previous research [30], which explored innovative techniques for revolutionizing contact lens manufacturing to improve both vision and comfort.

The performance of T-group CLs reflects a carefully balanced interaction between optical clarity, RI, and wearer comfort. The Si-NVP-HEMA copolymer matrix inherently provides a flexible, hydrophilic base with an elevated RI compared to traditional PHEMA, enhancing comfort through its rubbery texture and superior water retention. When ${\rm TiO_2}$ NPs are introduced, the high RI of these particles further increases

the overall RI, which can enhance visual acuity in certain applications. However, as ${\rm TiO_2}$ concentration decreases slightly, an interesting behavior emerges: the RI subtly increases, likely due to a refined interaction between the polymer and lower NP loads, which maintains clarity while subtly enhancing optical properties. Additionally, ${\rm TiO_2}$ dispersion within the Si-NVP-HEMA matrix is influenced by the hydrogen-bonding potential of NVP amide groups, which likely facilitates a uniform NP distribution. This reduces light scattering, even at higher ${\rm TiO_2}$ concentrations, as observed in T1 lenses, which achieve superior transmission with minimal scattering effects. This careful distribution, combined with Si-NVP-HEMA's hydrophilic properties, allows for a durable, hydrated lens that provides high clarity without compromising comfort or mechanical stability.

A-group CLs

The absorption spectra shown in Fig. 4a for A-group at varying concentrations from A1 to A5 reveal distinct trends. A notable observation is that as the concentration of Ag NPs decreases, the absorbance intensity increases. Specifically, A3 (1.32) and A4 (1.39) display the highest absorbance values, with A5 matching A4 intensity despite having a lower concentration. This unexpected increase in absorbance could be due to enhanced dispersion and reduced NP agglomeration, which allows for better light interaction. An anomalous behavior is seen in the A1 and A2 samples, where A1 has a higher Ag NP concentration than A2

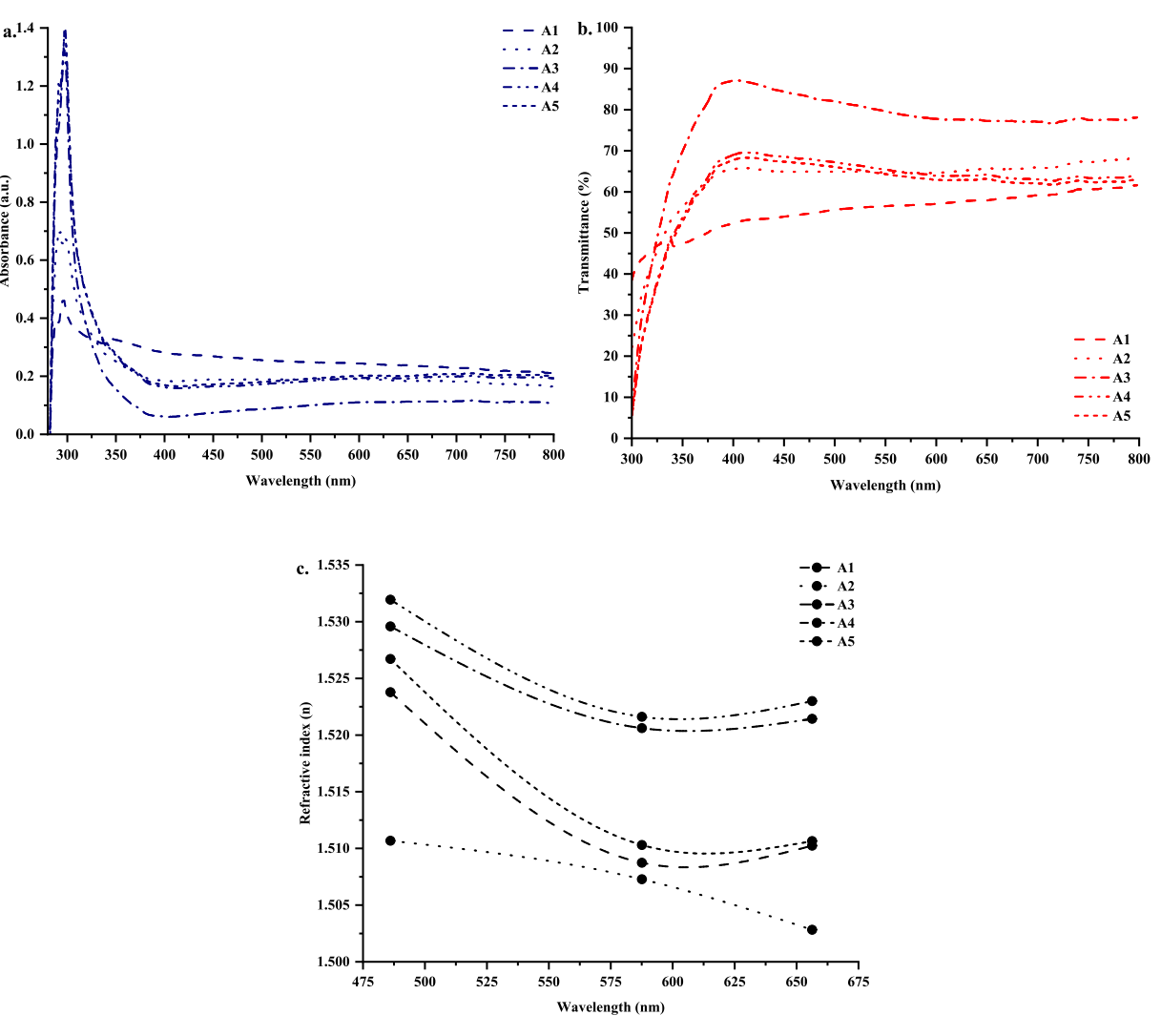


Fig. 4. (a) Uv-Vis absorption spectra, (b) transmission rate spectra, and (c) RI of A1-A5 CLs.

but demonstrates a lower absorbance intensity of 0.46 compared to 0.68 for A2. This behavior may result from clustering within the NPs in A1, which hinders uniform dispersion within the polymer matrix and limits the exposure of NPs to incident light. Consequently, the light absorption is reduced despite the higher concentration of Ag NPs.

The absorption peaks for A1-A5 CLs consistently appear around 297–297.50 nm, indicating stability in peak positioning. This stability suggests that the Si-based compounds present in the lens polymer do not significantly influence the absorption behavior of Ag NPs. Instead, the interaction appears to be primarily governed by the Ag NPs themselves, which maintain consistent peak absorption across samples. Larger Ag NPs, approximately 150 nm in size, likely exert a dominant influence on the optical properties of the lenses, as these particles exhibit strong absorbance. This absorbance effect may overshadow the optical contributions from Si-related compounds in the base polymer, positioning Ag NPs as the primary factor affecting the observed optical behavior.

Analyzing the transmission spectra depicted in Fig. 4b reveals how Ag NP concentration affects light passage through the lenses. A1 CL shows the lowest overall transmission across the visible spectrum. This low transmission is likely due to high concentration of Ag NPs, which enhances absorption and scattering properties, thus limiting the amount of light that can pass through the lens. A progressive increase in transmission is observed as the Ag NP concentration decreases from A2 to A5, suggesting that lower concentrations of Ag. This trend enables a larger amount of light to pass through the lenses, enhancing their overall transparency. The A3 sample, with a relatively low Ag NP concentration, demonstrates the highest transmission values, indicating an optimal balance of light passage with minimal absorbance. The presence of multiple peaks in the transmission spectra can be attributed to varying degrees of Ag NP aggregation and morphological changes, this is aligning with Albert et al. investigations [31]. The existence of nonspherical particles within aggregated Ag NPs may contribute to this phenomenon. The structural diversity of these particles results in different scattering and absorption responses, which manifest as multiple spectral peaks.

Regarding RI behavior shown in Fig. 4c, A-group CLs exhibited values ranging between 1.49 and 1.53 at different wavelengths. Interestingly, there is a subtle increase in RI as Ag NP concentration decreases, a trend like that observed in T-group. This increase in RI at lower Ag NP concentrations suggests that these concentrations favor a configuration that better supports higher refractive properties. the concentration of Ag NPs in the CLs profoundly influences their transmission and RI properties. Higher Ag NP concentrations correlate with increased light absorption and lower transmission, while lower concentrations favor greater transparency and higher RI. Although the polymer matrix and other materials contribute to optical behavior of CLs, Ag NP concentration remains the primary factor affecting transmission characteristics.

The combination of Si-NVP-HEMA and Ag NPs in CLs creates a synergistic effect that optimally balances optical performance, and protective qualities. Si-NVP-HEMA is inherently hydrophilic, enhancing water retention and promoting comfort by creating a moist surface on the lens. This hydrophilic property supports the well dispersion of Ag NPs, reducing the risk of aggregation, which is essential to maintain clarity and prevent excessive scattering. Where lower Ag NP concentrations allow higher light passage, while higher concentrations increase absorbance and scattering, impacting transparency [32]. Optically, Si-NVP-HEMA matrix has a moderate RI, while Ag NPs introduce variability, allowing the lens RI to be fine-tuned based on the concentration of NPs. This may decrease transmission due to greater light interaction as indicated recently by Madkhli A. Y. [33]. Si-NVP-HEMA matrix helps maintain Ag NP stability, allowing controlled RI adjustments without sacrificing clarity at optimal NP concentrations. Moreover, Ag NPs provide absorbance in specific UV and visible ranges, adding a layer of UV protection not inherent in Si-NVP-HEMA alone. This combination means the lens can offer both vision correction and UV filtering.

Mechanically, the flexible Si-NVP-HEMA structure contributes resilience and durability, while evenly distributed Ag NPs enhance the polymer network's stability.

Antibacterial activity

Fig. 5a–c show the Pure CL, T4, and A4 samples loaded with CAM and their SEM images. These images illustrated the loaded NPs to the front and back surfaces of CL. NPs, such as Ag and TiO₂, can affect the surface roughness of CLs. When incorporated into the lens material, these NPs can create microscopic irregularities that increase surface roughness [34]. Then, lenses need to be further polished, as shown by SEM images of the surface, to obtain smooth and comfortable lenses.

The antibacterial activity of the control (CAM), pure CL, T4, and A4, was evaluated against two bacterial strains, *S. aureus* and *E. coli* and recorded in Fig. 6. This type of bacteria is usually transmitted to the surface of the eye by touching contaminated materials, foods, and surfaces [35]. The control group using CAM exhibited moderate antibacterial activity against both *S. aureus* and *E. coli*, as reflected in inhibition zones of 7 mm and 11 mm, respectively. This highlights the inherent effectiveness of CAM in inhibiting bacterial growth.

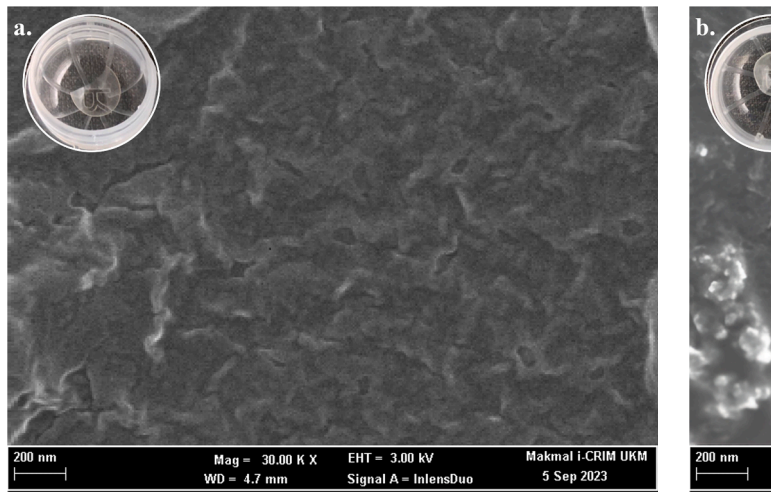
The pure CLs loaded with CAM demonstrated slightly larger inhibition zones compared to the control for both bacteria. For *S. aureus*, the mean inhibition zone increased to 8.13 ± 0.50 mm, which is approximately 16 % greater than the control. For *E. coli*, the mean inhibition zone was 12.03 ± 0.46 mm, representing an 8.90 % increase over the control. These results suggest that the pure CLs enhanced the localized delivery of CAM, improving its antibacterial efficacy slightly. [36]. This suggests that the polymer composite itself may have some inherent antibacterial properties, possibly due to the presence of CAM.

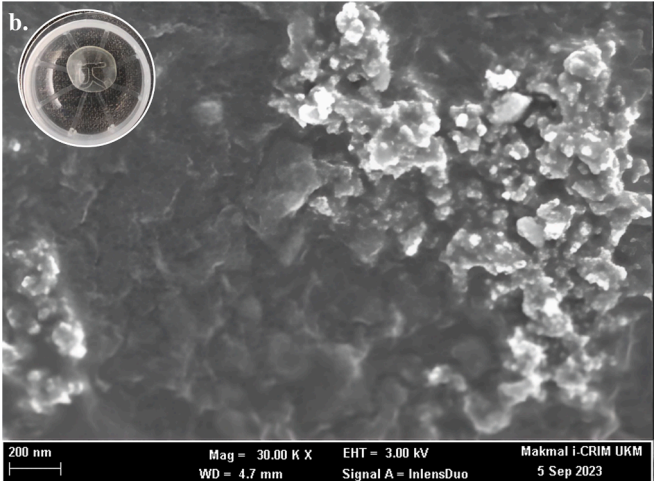
CAM-loaded T4, demonstrated moderate antibacterial activity against both bacterial strains, as reflected by inhibition zones of 12 ± 0.35 mm for *S. aureus* and 21.11 ± 0.52 mm for *E. coli*. While the antibacterial performance of T4 was not as pronounced as that of the A4 sample, it still showed statistically significant improvement compared to the control and pure lens. The inhibition zones for A4 were 14.03 ± 0.25 mm for *S. aureus* and 19.07 ± 0.31 mm for *E. coli*, surpassing the effectiveness of both T4 and pure lenses. The enhanced activity of A4 can be attributed to the antimicrobial synergy between CAM and the NPs, which act through multiple mechanisms, such as disruption of bacterial membranes (Ag NPs) and the generation of reactive oxygen species. This combination significantly improves bacterial inhibition.

The results indicate that the incorporation of Ag NPs and $\rm TiO_2$ NPs individually into the CLs, significantly enhances the antibacterial activity of the CL when compared to the control CAM and pure CL. The observed differences in inhibition zones suggest that the combined effects of CAM and NPs can provide a powerful tool for developing antibacterial CL materials, potentially reducing the risk of bacterial infections associated with CL wear. Further studies are warranted to explore the mechanisms underlying these enhanced antibacterial properties and their safety for ocular use. The mechanism of CAM drug release can be proposed regarding the physical interactions such as hydrogen bonding and van der Waals forces between CAM molecules and the eye fluid (tear film) [37]. Which would allow a small amount of CAM molecules to be released to the eye fluid. This will make a continuous release of drug from CLs.

Water content analysis and oxygen permeability measurement

Oxygen permeability is a crucial characteristic of CLs as it directly affects the ability of cornea to receive adequate oxygen, which is essential for maintaining corneal metabolism and overall eye health. Insufficient oxygen transmission can lead to hypoxia [38], resulting in complications such as corneal swelling, neovascularization [39], and discomfort [40]. Starting with Table 2, when the outer surfaces of T-group, the water content decreased from approximately 81 % to around





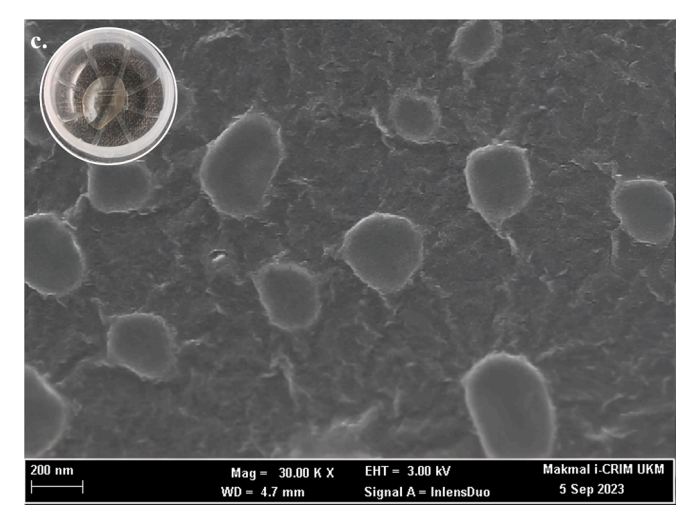


Fig. 5. (a) pure, (b) T4, and (c) A4 CLs samples loaded with CAM their SEM images.

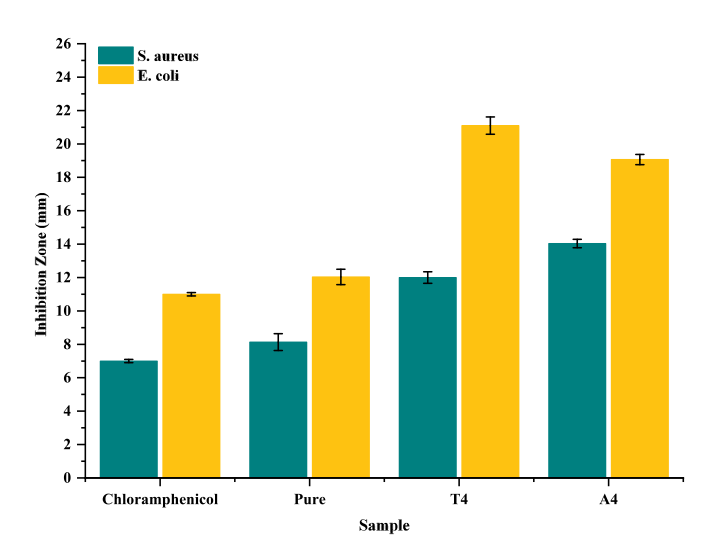


Fig. 6. The inhibition zones measured in millimeters against two bacterial strains, *S. aureus* and *E. coli*.

73 % due to a slight reduction in the polymer's porosity. However, the water content increased as TiO_2 NPs concentration increased from T5 to T1, gradually rising from approximately to about 78 %. This suggests that TiO_2 NPs exhibit a hydrophilic property [41]. Regarding oxygen permeability, it decreased directly from 41 to approximately 31 barrers

when ${\rm TiO_2}$ NPs have been loaded. Then, the oxygen permeability increased as the NPs concentration increased from T5 to T1 approached about 38 barrers due to the larger surface area-to-volume ratio, allowing for a greater amount of oxygen to pass through the water. The initial loading of CLs with ${\rm TiO_2}$ NPs of approximately 21 nm size resulted in a decrease in water content, while increasing the concentration of these NPs led to higher water content. The oxygen permeability initially decreased with ${\rm TiO_2}$ NP loading but increased as the NP concentration rose, indicating a complex interplay between oxygen permeability, water content, and corneal health.

When loading the inner surfaces of the CLs with Ag NPs, the water content of the CLs decreased, as illustrated in Table 3. However, in

Table 3 The relationship between the concentration of Ag and ${\rm TiO_2}$ NPs and the EWC as well as gas permeability of the CLs.

Sample	Dry (g)	Wet (g)	EWC (%)	DK (barrer)	DK/t (barrer/mm)
Pure	0.014	0.073	80.82	41.32	413.20
T1 CL	0.014	0.065	78.78	38.11	381.10
T2 CL	0.015	0.070	78.57	37.79	377.90
T3 CL	0.016	0.070	77.14	35.70	357.00
T4 CL	0.018	0.070	74.28	31.87	318.70
T5 CL	0.019	0.072	73.61	31.03	310.30
A1 CL	0.016	0.063	74.60	32.28	322.80
A2 CL	0.016	0.063	74.60	32.28	322.80
A3 CL	0.017	0.077	77.92	36.83	368.30
A4 CL	0.017	0.080	78.75	38.06	380.60
A5 CL	0.017	0.082	79.26	38.85	388.50

L.M. Shaker et al. Results in Chemistry 13 (2025) 102034

contrast to loading $\rm TiO_2$ NPs, CLs loaded with Ag NPs exhibited contrasting behavior. The water content gradually decreased from approximately 79 % to about 74 % as the concentration of Ag NPs increased [42]. Nevertheless, due to Ag's strong hydrophilic property, all CLs retained approximately 74–79 % of their water content. The relatively large size of Ag NPs, around 150 nm, played a role in reducing the amount of permeating oxygen, which the CLs can hold and transmit to the cornea. As the concentration of Ag increased from A5 to A1, the oxygen permeability decreased from approximately 38 to 32 barrers, respectively. Loading hydrophilic Ag NPs into CLs can increase water content, provide antimicrobial benefits, but may also impact oxygen permeability. Balancing these factors is essential to ensure that the lenses remain comfortable, safe, and suitable for long-term wear.

FT-IR analysis

FT-IR chart corresponds to a synthesized contact material composed of NVP, HEMA, and TEOS loaded with CAM. By analyzing the FT-IR peaks shown in Fig. 7, we can gain valuable insights into the chemical composition and functional groups present within this material. These peaks reflect the characteristic vibration bands associated with the molecular vibrations of NVP, HEMA, and TEOS, as well as the incorporation of CAM. For instance, the presence of specific peaks could indicate the successful formation of siloxane bonds from TEOS, the ester linkages from HEMA, and the amide groups from NVP. Additionally, any shifts or changes in the intensity of these peaks might suggest interactions between CAM and the polymer matrix, providing further understanding of how the antibiotic is integrated and stabilized within the material. CAM Loaded-Pure CL curve, peaks at 3394 cm⁻¹ indicate O-H stretching vibrations, suggesting the presence of hydroxyl groups from HEMA or silica formed from TEOS. Peaks at 2958 cm⁻¹ and 1720 cm⁻¹ are associated with C-H and C=O stretching vibrations, indicating organic compounds like PVP and HEMA, and carbonyl groups possibly from HEMA, respectively. Additionally, peaks at 1651 cm⁻¹ and 1462 cm⁻¹ could be attributed to amide and aromatic or alkene groups, further confirming the composition. In the CAM Loaded-T4 curve peaks at 3389 cm⁻¹ and 2957 cm⁻¹ suggest the presence of hydroxyl and C-H stretching vibrations, possibly from TEOS and organic compounds like PVP and HEMA, respectively. Peaks at 1720 cm⁻¹ and 1650 cm⁻

indicate the presence of carbonyl and amide groups, suggesting the composition includes HEMA and PVP. The peaks at $1289~\rm cm^{-1}$ and $923~\rm cm^{-1}$ may be related to Si-O-Si and Si-O-Ti vibrations, indicating the incorporation of TEOS-derived silica and $\rm TiO_2$ NPs, if present. From the same figure, CAM Loaded-A4 curve have shown clear peaks at $3395~\rm cm^{-1}$ and $2985~\rm cm^{-1}$ suggest the presence of hydroxyl and C-H stretching vibrations, possibly from various sources including TEOS, HEMA, or CAM. Peaks at $1720~\rm cm^{-1}$ and $1651~\rm cm^{-1}$ indicate the presence of carbonyl and amide groups, suggesting the composition includes HEMA, PVP, or CAM. The presence of peaks at $1167~\rm cm^{-1}$ and $1020~\rm cm^{-1}$ could be attributed to Ag-O or Ag-N bonds and Ag NPs, indicating the successful loading of silver NPs. The peaks at $754~\rm cm^{-1}$ and $684~\rm cm^{-1}$ may be associated with Si-O-Ti vibrations and metal–oxygen bonds, indicating interactions between the silica network, Ag NPs, and CAM.

Conclusions

The present study demonstrated that Si-NVP-HEMA-based CLs, loaded with antibacterial agents such as CAM, TiO2 NPs, and Ag NPs, offer enhanced antimicrobial efficacy compared to standard Pure CL. Si-NVP-HEMA proved to be an effective polymer matrix, capable of uniformly incorporating these agents while maintaining their stability and facilitating a controlled release over time. The T4 sample, containing TiO2 NPs, exhibited moderate antibacterial activity, attributable to the photocatalytic properties of TiO2. The A5 sample, loaded with Ag NPs, displayed superior antibacterial effectiveness due to the broad-spectrum antimicrobial nature of silver. Notably, lenses incorporating both TiO2 and Ag NPs showed the highest antibacterial activity, suggesting a synergistic effect when used in conjunction with CAM. These results underscore the potential of Si-NVP-HEMA as a robust platform for antibacterial CL development, with the combined presence of CAM and NPs significantly reducing the risk of bacterial infections for lens wearers. Further research should investigate the release mechanisms of these agents within the Si-NVP-HEMA matrix and evaluate the longterm safety and ocular compatibility of these advanced antibacterial CLs to ensure they meet the standards for daily wear.

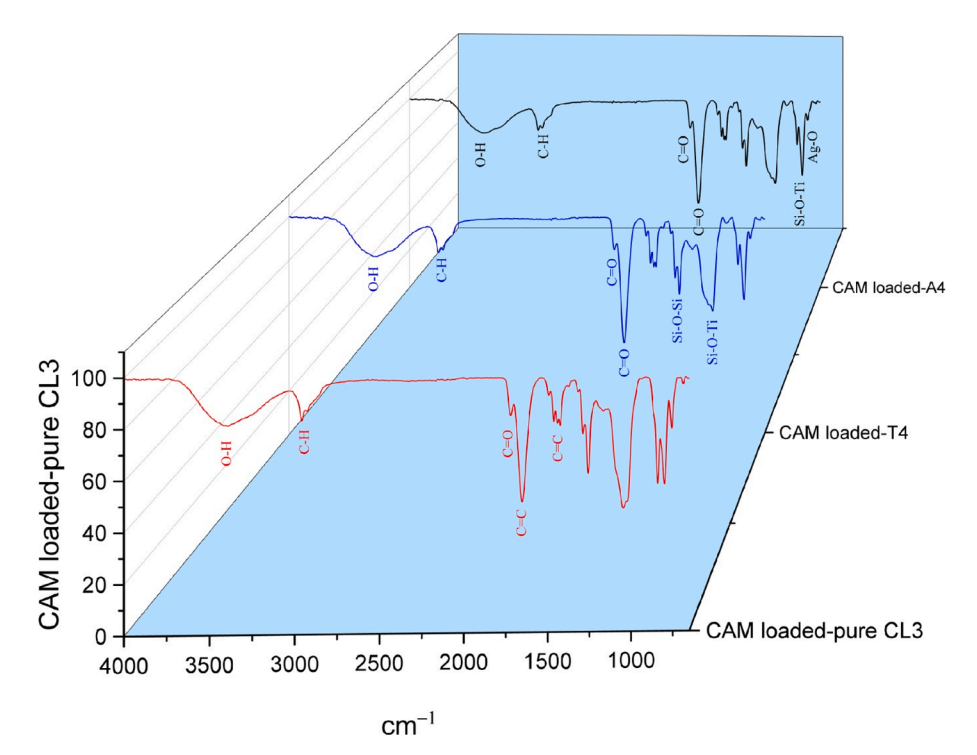


Fig. 7. FT-IR of CAM loaded-pure, CAM loaded-T4, and CAM loaded-A4 CLs.

L.M. Shaker et al. Results in Chemistry 13 (2025) 102034

To conclude, the novelty of this study lies in its integrated approach that combines advanced material science, antimicrobial properties, and optical performance, potentially offering a safer, more comfortable, and functional option for extended-wear CL users. The primary sustainable development goal (SDG) aligned with this research is SDG 3: Good Health and Well-being, given its focus on improving ocular health and reducing infection risks associated with CLs without compromising optical performance. By integrating antimicrobial agents into the lens matrix, this work not only advances innovative healthcare solutions but also has the potential to improve public health outcomes by making CLs safer for users. Furthermore, this research contributes to SDG 9: Industry, Innovation, and Infrastructure by advancing the development of multifunctional medical devices and holds promise for sustainable production practices in the medical and optical industries, aligning with SDG 12: Responsible Consumption and Production.

CRediT authorship contribution statement

Lina M. Shaker: Writing – original draft, Resources, Project administration, Methodology, Investigation, Formal analysis, Conceptualization. **Ahmed Alamiery:** Writing – review & editing, Supervision, Project administration, Methodology, Investigation, Funding acquisition, Conceptualization. **Abdulamier Ahmed Abdulamier:** Writing – original draft, Visualization, Resources, Data curation. **Wan Nor Roslam Wan Isahak:** Writing – review & editing, Resources, Project administration.

Declaration of competing interest

The authors declare that they have no known competing financial interests or personal relationships that could have appeared to influence the work reported in this paper.

Acknowledgments

The authors gratefully acknowledge Al-Ayen Iraqi University and the Universiti Kebangsaan Malaysia for providing the financial support through grant code TT-2023-018, which made this research possible.

Data availability

Data will be made available on request.

References

- N. Tahhan, T.J. Naduvilath, C. Woods, E. Papas, Review of 20 years of soft contact lens wearer ocular physiology data, Cont. Lens Anterior Eye 45 (2022) 1–18, https://doi.org/10.1016/j.clae.2021.101525.
- [2] P. Mehta, R. Haj-Ahmad, A. Al-Kinani, M.S. Arshad, M.W. Chang, R.G. Alany, Z. Ahmad, Approaches in topical ocular drug delivery and developments in the use of contact lenses as drug-delivery devices, Ther. Deliv. 8 (2017) 521–541, https:// doi.org/10.4155/tde-2017-0018.
- [3] A. Chandel, G. Kandav, Insights into ocular therapeutics: a comprehensive review of anatomy, barriers, diseases and nanoscale formulations for targeted drug delivery, J. Drug Deliv. Sci. Technol. 97 (2024) 105785, https://doi.org/10.1016/ JJDDST.2024.105785.
- [4] Z. Wang, X. Li, X. Zhang, R. Sheng, Q. Lin, W. Song, L. Hao, Novel contact lenses embedded with drug-loaded zwitterionic nanogels for extended ophthalmic drug delivery, Nanomaterials 11 (2021), https://doi.org/10.3390/nano11092328.
- [5] J.H. Bae, B. Choi, Y.J. Kim, H.M. Lee, K.H. Kim, Y.S. Han, Preparation and physical properties of a silicone hydrogel contact lens grafted with a phosphorylcholinecontaining hydrophilic copolymer, Macromol. Res. 30 (2022) 446–453, https:// doi.org/10.1007/s13233-022-0046-4.
- [6] Q. Zhu, S. Mao, Enhanced drug loading efficiency of contact lenses via salt-induced modulation, Asian, J. Pharm. Sci. 14 (2019) 204–215, https://doi.org/10.1016/j. aips.2018.05.002.
- [7] L. Zhao, J. Song, Y. Du, C. Ren, B. Guo, H. Bi, Therapeutic applications of contact lens-based drug delivery systems in ophthalmic diseases, Drug Deliv. 30 (2023), https://doi.org/10.1080/10717544.2023.2219419.
- [8] E.M. Rueff, Visual discomfort and contact lens wear: a review, Cont. Lens Anterior Eye 46 (2023), https://doi.org/10.1016/j.clae.2023.101872.

[9] D. Costa, V. De Matteis, F. Treso, G. Montani, M. Martino, R. Rinaldi, M. Corrado, M. Cascione, Impact of the physical properties of contact lens materials on the discomfort: role of the coefficient of friction, Colloids Surf. B Biointerfaces 233 (2024), https://doi.org/10.1016/j.colsurfb.2023.113630.

- [10] C.H. Tam, M.S. Alexander, J. Sanderson, S. Qi, Selectively coated contact lenses by nanoelectrospray (nES) to fabricate drug-eluting contact lenses for treating ocular diseases, Med. Eng. Phys. 124 (2024), https://doi.org/10.1016/j. medengphy.2024.104110.
- [11] M. Contardi, D. Kossyvaki, P. Picone, M. Summa, X. Guo, J.A. Heredia-Guerrero, D. Giacomazza, R. Carzino, L. Goldoni, G. Scoponi, F. Rancan, R. Bertorelli, M. Di Carlo, A. Athanassiou, I.S. Bayer, Electrospun polyvinylpyrrolidone (PVP) hydrogels containing hydroxycinnamic acid derivatives as potential wound dressings, Chem. Eng. J. 409 (2021), https://doi.org/10.1016/j.cej.2020.128144.
- [12] P.J. Bora, A.G. Anil, P.C. Ramamurthy, Y.H. Lee, Chemically room temperature crosslinked polyvinyl alcohol (PVA) with anomalous microwave absorption characteristics, Macromol. Rapid Commun. 42 (2021) 2000763, https://doi.org/ 10.1002/marc.202000763.
- [13] M.S.B. Husain, A. Gupta, B.Y. Alashwal, S. Sharma, Synthesis of PVA/PVP based hydrogel for biomedical applications: a review, Energy Sources Part A 40 (2018) 2388–2393, https://doi.org/10.1080/15567036.2018.1495786.
- [14] P. Boonsuk, K. Kaewtatip, S. Chantarak, A. Kelarakis, C. Chaibundit, Super-tough biodegradable poly(vinyl alcohol)/poly(vinyl pyrrolidone) blends plasticized by glycerol and sorbitol, J. Appl. Polym. Sci. 135 (2018) 1–8, https://doi.org/ 10.1002/app.46406.
- [15] K.A. Juby, C. Dwivedi, M. Kumar, S. Kota, H.S. Misra, P.N. Bajaj, Silver nanoparticle-loaded PVA/gum acacia hydrogel: Synthesis, characterization and antibacterial study, Carbohydr. Polym. 89 (2012) 906–913, https://doi.org/ 10.1016/j.carbpol.2012.04.033.
- [16] M. Afshar, G. Dini, S. Vaezifar, M. Mehdikhani, B. Movahedi, Preparation and characterization of sodium alginate/polyvinyl alcohol hydrogel containing drugloaded chitosan nanoparticles as a drug delivery system, J. Drug. Deliv. Sci. Technol. 56 (2020), https://doi.org/10.1016/j.jddst.2020.101530.
 [17] Z.A. Abdul Muhsin, A.S. Aldhamin, S.S. Shafik, Enhancement mechanical
- [17] Z.A. Abdul Muhsin, A.S. Aldhamin, S.S. Shafik, Enhancement mechanical properties of cellulose ethers-polyvinyl alcohol blend by uv irradiation, Iran J. Ichthyol. 8 (2021) 168–176.
- [18] P. Zhao, J. Xu, Y. Zhang, W. Zhu, Y. Cui, Polymerizable-group capped ZnS nanoparticle for high refractive index inorganic-organic hydrogel contact lens, Mater. Sci. Eng. C 90 (2018) 485–493, https://doi.org/10.1016/j.msec.2018.04.086.
- [19] S. Kennedy, J.G. Linhardt, A. Diciccio, Cast Moldable, High RI, Rigid, Gass Permeable polymer formulations for an Accommodating Contact Lens, U.S Patent 0088352 A1, March 29, 2018.
- [20] J. Schafer, W. Reindel, R. Steffen, G. Mosehauer, J. Chinn, Use of a novel extended blink test to evaluate the performance of two polyvinylpyrrolidone- containing, silicone hydrogel contact lenses, Dovepress j, Clin. Ophthalmol. 12 (2018) 819–825. https://doi.org/10.2147/OPTH.S162233.
- [21] R.K. Gupta, M.A. Alzayed, A.A. Aba Alkhayl, T.S. Bedaiwi, Effect of light sources on transmittance of commercially available contact lenses, Cureus (2024), https://doi. org/10.7759/cureus.62093.
- [22] L.M. Shaker, W.K. Al-Azzawi, A. Al-Amiery, M.S. Takriff, W.N.R. Wan Isahak, Highly transparent antibacterial hydrogel-polymeric contact lenses doped with silver nanoparticles, J. Vinyl Add. Technol. 29 (2023) 1023–1035, https://doi.org/ 10.1002/ynl.21995
- [23] A.A. Abdulamier, L.M. Shaker, A.A. Al-Amiery, Advancements in the chemistry of contact lenses: innovations and applications, Results Chem. 12 (2024) 101872, https://doi.org/10.1016/J.RECHEM.2024.101872.
- [24] L.M. Shaker, A. Al-Amiery, W.N.R.W. Isahak, W.K. Al-Azzawi, Vinyl polymers as key materials in contact lens design: a review of progress and future directions, Starch/Staerke 76 (2024), https://doi.org/10.1002/star.202300213.
- [25] M. Mahjoob, S. Heydarian, Effect of contact lenses on contrast sensitivity under various lighting conditions, J. Ophthalmic Vis. Res. 16 (2021) 538–543, https://doi.org/10.18502/JOVR.V1614.9742.
- [26] N. Efron, Contact Lens Practice E-Book, 3rd ed., Elsevier Health Sciences, 2016.
- [27] E.B. Papas, The significance of oxygen during contact lens wear, Cont. Lens Anterior Eye 37 (2014) 394–404, https://doi.org/10.1016/j.clae.2014.07.012.
- [28] R.N. Abed, M. Abdallh, A. Adnan Rashad, H.C. Al-Mohammedawi, E. Yousif, Spectrally selective coating of nanoparticles (Co3O4:Cr2O3) incorporated in carbon to captivate solar energy, Heat Transfer 49 (2020) 1386–1401, https://doi. ore/10.1002/hti.21668.
- [29] F.S. Ansari, S. Daneshjou, Optimizing the green synthesis of antibacterial TiO2 anatase phase nanoparticles derived from spinach leaf extract, Sci. Rep. 14 (2024) 22440, https://doi.org/10.1038/s41598-024-73344-5.
- [30] L.M. Shaker, A. Al-Amiery, W.N.R. Wan Isahak, Revolutionizing contact lens manufacturing: exploring cutting-edge techniques and innovations for enhanced vision and comfort, Int. J. Low-Carbon Technol. 19 (2024) 359–385, https://doi. org/10.1093/iiict/ctadl.36
- [31] H.M. Albert, K. Mendam, P.G. Bansod, M.S.S. Rao, A. Asatkar, M.K. Chakravarthi, M.P. Mallesh, Biosynthesis, spectroscopic, and antibacterial investigations of silver nanoparticles, J. Fluoresc. (2023), https://doi.org/10.1007/s10895-023-03398-7.
- [32] L. Chronopoulou, R. Binaymotlagh, S. Cerra, F.H. Haghighi, E.G. Di Domenico, F. Sivori, I. Fratoddi, S. Mignardi, C. Palocci, Preparation of hydrogel composites using a sustainable approach for in situ silver nanoparticles formation, Materials 16 (2023), https://doi.org/10.3390/ma16062134.
- [33] A.Y. Madkhli, Effect of adding methyl orange/silver (MO-Ag) nanoparticles on the optical and structural properties of polyvinyl alcohol (PVA), Opt. Quant. Electron. 56 (2024), https://doi.org/10.1007/s11082-023-05843-0.

- [34] S. Chupradit, M. Kavitha, W. Suksatan, M.J. Ansari, Z.I. Al Mashhadani, M. M. Kadhim, Y.F. Mustafa, S.S. Shafik, E. Kianfar, Morphological control: properties and applications of metal nanostructures, Adv. Mater. Sci. Eng. 2022 (2022), https://doi.org/10.1155/2022/1971891.
- [35] H. Agha, A.B. Sanaalla, M.A.S. Abdulsamad, M. abderrahmane Salhi, G.A.-R. Mohammad, A.A.A. Allaq, Impact of Some Parameters on the Survival and Proliferation of Foodborne Pathogens: Escherichia coli, Bacillus subtilis, Staphylococcus aureus, and Streptococcus pyogenes, AUIQ Complementary Biological System 1 (2024) 70–76. doi: 10.70176/3007-973x.1007.
- [36] J.S. Wolffsohn, K. Dumbleton, B. Huntjens, H. Kandel, S. Koh, C.M.E. Kunnen, M. Nagra, H. Pult, A.L. Sulley, M. Vianya-Estopa, K. Walsh, S. Wong, F. Stapleton, CLEAR - evidence-based contact lens practice, Cont. Lens Anterior Eye 44 (2021) 368–397, https://doi.org/10.1016/j.clae.2021.02.008.
- [37] Q. Wang, A. Zhang, L. Zhu, X. Yang, G. Fang, B. Tang, Cyclodextrin-based ocular drug delivery systems: a comprehensive review, Coord. Chem. Rev. 476 (2023), https://doi.org/10.1016/j.ccr.2022.214919.

- [38] C.C. Jensen, N.A. Warfel, Hypoxia, in: Comprehensive Pharmacology, Elsevier, 2022: pp. 438–468. doi: 10.1016/B978-0-12-820472-6.00039-6.
- [39] M. Economopoulou, H.F. Langer, A. Celeste, V.V. Orlova, E.Y. Choi, M. Ma, A. Vassilopoulos, E. Callen, C. Deng, C.H. Bassing, M. Boehm, A. Nussenzweig, T. Chavakis, Histone H2AX is integral to hypoxia-driven neovascularization, Nat. Med. 15 (2009) 553–558, https://doi.org/10.1038/nm.1947.
- [40] F. Stapleton, J. Tan, Impact of contact lens material, design, and fitting on discomfort, Eye Contact Lens. 43 (2017) 32–39, https://doi.org/10.1097/ ICL.0000000000000318.
- [41] Y. Kameya, H. Yabe, Optical and superhydrophilic characteristics of TiO2 coating with subwavelength surface structure consisting of spherical nanoparticle aggregates, Coatings 9 (2019), https://doi.org/10.3390/coatings9090547.
- [42] Z. Yang, H. Guo, Z.K. Yao, Y. Mei, C.Y. Tang, Hydrophilic silver nanoparticles induce selective nanochannels in thin film nanocomposite polyamide membranes, Environ. Sci. Technol. 53 (2019) 5301–5308, https://doi.org/10.1021/acs. est.9b00473.